Journal of Advanced Ceramics
2014, 3(4): 297–305
DOI: 10.1007/s40145-014-0121-1

ISSN 2226-4108
CN 10-1154/TQ

Research Article

Investigation of strong shock wave interactions with CeO_2 ceramic

Vishakantaiah JAYARAM[a,*], Asha GUPTA[b], K. P. J. REDDY[c]

[a]*Shock Induced Materials Chemistry Lab*, *SSCU*, *Indian Institute of Science*, *Bangalore-560012*, *India*
[b]*Texas Materials Institute*, *the University of Texas at Austin*, *Austin*, *Texas 78712*, *USA*
[c]*Department of Aerospace Engineering*, *Indian Institute of Science*, *Bangalore-560012*, *India*

Received: April 05, 2014; Revised: July 16, 2014; Accepted: July 23, 2014

Abstract: Strong shock wave interactions with ceramic material ceria (CeO_2) in presence of O_2 and N_2 gases were investigated using free piston driven shock tube (FPST). FPST is used to heat the test gas to very high temperature of about 6800–7700 K (estimated) at pressure of about 6.8–7.2 MPa for short duration (2–4 ms) behind the reflected shock wave. Ceria is subjected to super heating and cooling at the rate of about 10^6 K/s. Characterization of CeO_2 sample was done before and after exposure to shock heated test gases (O_2 and N_2). The surface composition, crystal structure, electronic structure and surface morphology of CeO_2 ceramic were examined using X-ray photoelectron spectroscopy (XPS), X-ray diffraction (XRD), Fourier transform infrared (FTIR) spectrometry, scanning electron microscopy (SEM) and high resolution transmission electron microscopy (HRTEM). Results obtained from the experimental investigations show that CeO_2 can withstand high pressure accompanied by thermal shock without changing its crystal structure. Reducible CeO_2 releases lattice oxygen making it possible to shift between reduced and oxidized states upon the interaction with shock heated gas. Due to such reaction mechanism, CeO_2 ceramic undergoes nitrogen doping with decrease in lattice parameter. Investigations reveal that CeO_2 retains its crystal structure during strong shock interaction, even at elevated pressure.

Keywords: shock tube; shock interaction; high enthalpy gas; ceria; nitrogen-doped; surface reaction

1 Introduction

Ceria based materials have been explored for several applications such as heterogeneous catalysis [1,2], gas sensors [3], fuel cells [4], bio-materials [5,6], bio-photonics [7], etc. In many applications, knowledge of the cerium oxidation state is necessary for understanding the properties of the ceria compounds. These ceria based catalysts are very useful as high temperature materials for space applications and also for three-way catalysis. Among rare earth oxides, CeO_2 ceramic material draws special attention due to its role as a promoter for the control of toxic emission from automobile exhaust for many years. Ceria is usually treated as an active support for precious metal as well as base metal catalyst in heterogeneous catalysis. Reducible CeO_2 can release lattice oxygen making it possible to shift between reduced and oxidized states ($Ce^{4+}(4f^0) \leftrightarrow Ce^{3+}(4f^1)$) indicating high endurance of ceria towards fluctuating oxygen vacancies under oxygen excess and deficient conditions. The extent of lattice oxygen that can be released and restored is known as "oxygen storage capacity (OSC)" [8]. This unique property of ceria has

* Corresponding author.
E-mail: jayaram@sscu.iisc.ernet.in, drjayaramv@gmail.com

made it a special component for three-way catalyst since it can store oxygen during oxygen-lean conditions and release oxygen during oxygen-rich conditions. Under oxygen-rich condition, cerium ion is in 4+ oxidation state, and reduces partially to 3+ oxidation state under oxygen-lean condition. In addition, ceria keeps the same cubic crystal structure even during the alternate storage and release of oxygen and its volume change is observed to be very small.

Stoichiometric CeO_2 has a cubic fluorite lattice (space group *Fm*3*m*) with four cerium and eight oxygen atoms per unit cell. The Ce^{4+} cations occupy the face centered cubic lattice sites, and the oxygen anions (O^{2-}) are located at the eight tetrahedral sites. From structural considerations, the addition or removal of oxygen atoms should involve a minimal reorganization of the skeleton arrangement of the cerium atoms [9,10]. This structural property should definitely facilitate the excellent reversibility of the reduction–oxidation process. The unit cell is constructed out of eight unit cells of CeO_2 with 25% of the oxygen vacancies created in a particular arrangement and the cations are six coordinated [11]. High pressure study of bulk CeO_2 at room temperature shows phase transformation from cubic fluorite to orthorhombic phase on the application of 35 GPa pressure. Study at higher temperature (1473 K) at 14.5 GPa shows similar phase transformation, but at room temperature on decompression it comes back to cubic fluorite structure [12].

Free piston driven shock tube (FPST) which is a part of hypersonic shock tunnel 3 (HST3) has been used to investigate the effect of strong shock compression on several nano materials [13–16]. Thermal protection system (TPS) materials are generally tested in presence of air for space applications. In general, shock heated O_2 and N_2 (instead of air) gases are used to study aerothermodynamic reactions during re-entry of space vehicles. Studies of oxidation and nitridation reactions are essential to understand the catalytic activity of high temperature ceramic materials. The novel methods of investigating the interaction of real gases with the materials for short duration using shock tubes are not reported in the literature. In this paper we report one such study where we present the experimental results obtained on the interaction of CeO_2 with strong shock heated O_2 and N_2 gases for short duration (2–4 ms) using FPST.

2 Experimental methods

Ceria ceramic nanopowders were synthesized by the solution combustion method to study their behavior on shock loading. Experiments were performed on CeO_2 using shock heated O_2 and N_2 at high temperature and pressure. High enthalpy thermodynamic conditions generated in FPST were utilized to investigate the shock interaction behavior of CeO_2. The characterization of CeO_2 was carried out before and after the interaction with shock heated test gases using different experimental methods.

2.1 Solution combustion synthesis of nanopowders of ceramic material CeO_2

CeO_2 was synthesized by the solution combustion method [17]. The chemical combustion reaction led to the formation of solid oxide by using 5.4826 g (0.01 mol) of ammonium cerium (IV) nitrate $(NH_4)_2Ce(NO_3)_6{\cdot}6H_2O$ and 1.98 g (0.01 mol) of glycine ($C_2H_5NO_2$) dissolved in distilled water, taken in a crystallizing dish. The compounds were dissolved into clear solution. The solution was rapidly heated in a furnace at 723 K. After dehydration, the solution was ignited into a flame, rising the temperature to about 1273 K for 1–2 min, leaving behind pale yellow color nanocrystalline ceramic powders of CeO_2 as per the following chemical equation:

$$3(NH_4)_2Ce(NO_3)_6 + 8C_2H_5NO_2 \rightarrow 3CeO_2 + 16CO_2 + 16N_2 + 32H_2O$$

Nanocrystalline ceramic powders were then made into pellets using hydraulic press unit by applying 75 kN load before exposing to shock heated test gases. Pellets were made by using 0.2 g CeO_2. Synthesized CeO_2 was exposed to strong shock heated oxygen and nitrogen gases using FPST.

2.2 Experimental facilities and conditions of test gases

FPST consists of a high pressure gas reservoir, compression tube filled with driver gas (helium for the present study) and shock tube with a provision to mount the test sample on the end flange. Operation of the FPST involves placing the piston at mounting location of the gas reservoir and holding it rigidly by vacuum after evacuation. Aluminum diaphragm is placed in between the compression tube filled with helium gas at 1 atm and the shock tube. After evacuating the shock tube, gas handling system is used

to fill the test gas at a required pressure. Ultra-high pure (UHP) O_2 or N_2 is purged many times. The shock tube is initially evacuated using vacuum pump and then filled with test gas (O_2 or N_2) at required pressure. Sudden supply of the high pressure gas by opening valves behind the piston sets its motion in the compression tube and as a result, the piston gets maximum acceleration. Motion of 20 kg piston in compression tube adiabatically compresses the helium gas and thereby increases the pressure and temperature. This high pressure and high temperature helium gas bursts the primary diaphragm. It produces a normal primary shock wave, traveling into the driven section of a shock tube filled with test gas, which is reflected finally at the end of the shock tube to generate higher stagnation temperature and pressure. The reflected shock wave can be used to produce a stagnation enthalpy of about 10 MJ/kg. A simple working principle of FPST was described in earlier references [18,19]. Detail experimental procedure, working condition and development of the FPST were described elsewhere [20,21]. The schematic diagram of FPST is shown in Fig. 1. The panoramic view of the completely assembled 21 m long FPST (HST3) is shown in Fig. 2.

The temperature behind the reflected shock wave (T_5)

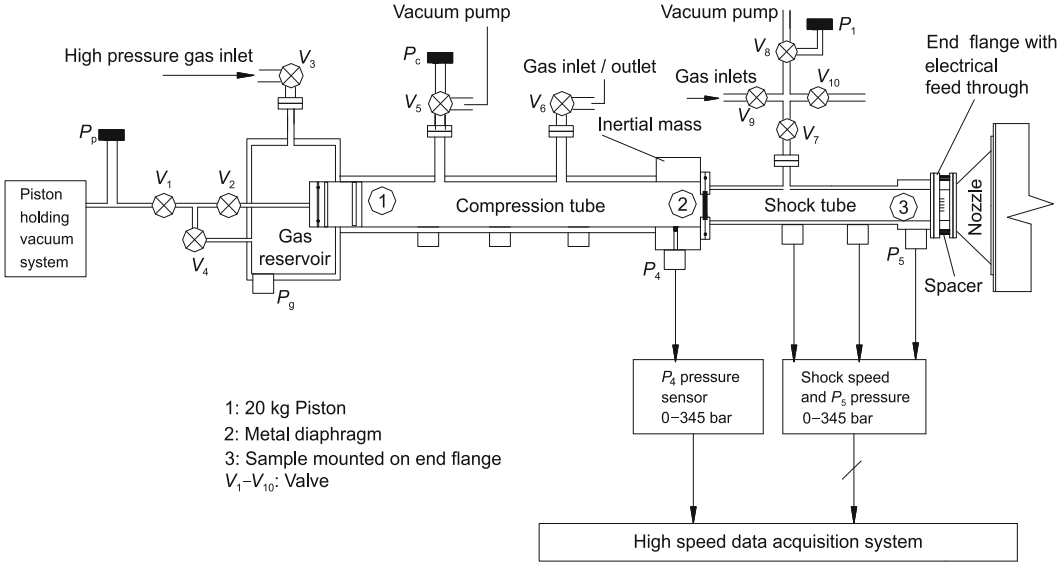

Fig. 1 Schematic diagram of FPST.

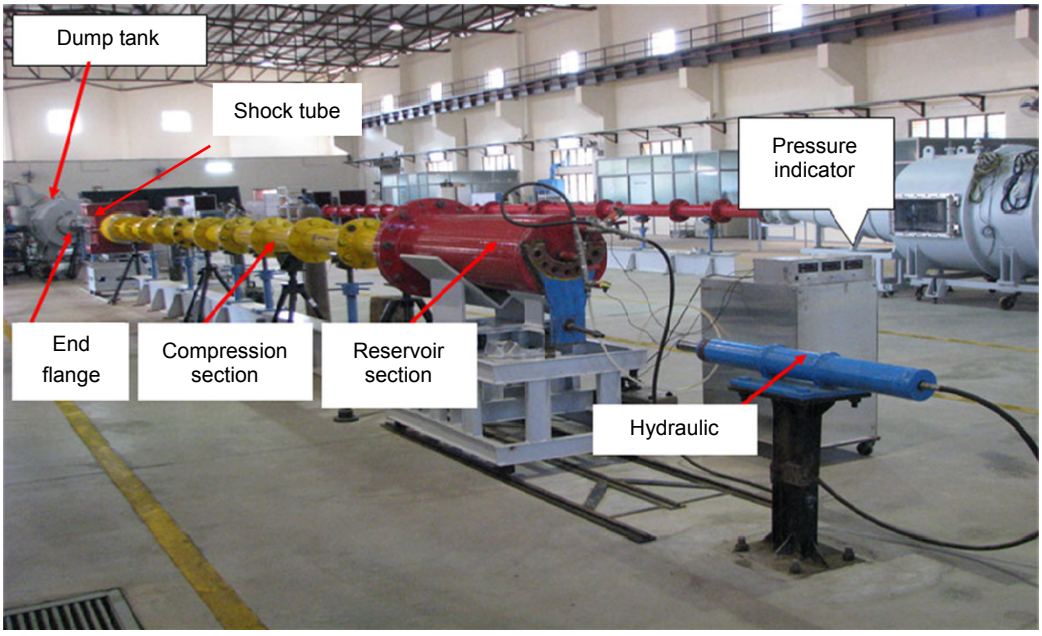

Fig. 2 Panoramic view of completely assembled 21 m long FPST.

and the corresponding specific enthalpy of the test gas at the end of the shock tube are estimated using normal shock relation [22]:

$$\frac{T_5}{T_1} = \frac{[2(\gamma-1)M_s^2+(3-\gamma)][(3\gamma-1)M_s^2-2(\gamma-1)]}{(\gamma+1)^2 M_s^2}$$

where γ is the specific heat ratio of the test gas; M_s is the measured shock Mach number; and T_1 is the initial temperature of the test gas in the shock tube.

Experiments were performed by filling helium gas at 0.1 MPa in the compression tube while shock tube was filled with test gas at initial pressure of 0.01 MPa. The shock heated O_2 test gas was made to react for 2–4 ms with the CeO_2 pellets mounted on the end flange of the shock tube. Typical experimentally measured and recorded parameters are shock speed 2440 m/s corresponding to shock Mach number of 6.9 and reflected shock pressure ~6.8 MPa. Hence in this experiment, the sample was subjected to the reflected shock pressure of 6.8 MPa measured using pressure sensor mounted at the end of the shock tube and estimated reflected shock temperature of about 6400 K for about 2–4 ms. Similar experimental conditions were set for nitrogen test gas with corresponding values of 2630 m/s shock speed, 7.4 shock Mach number and reflected shock pressure 7.2 MPa, at estimated reflected shock temperature of about 7700 K. The typical shock speed and reflected shock pressure signals have been recorded by using piezoelectric pressure transducer, as shown in Figs. 3(a) and 3(b), respectively. The ceramic test compound was mounted at the end of the shock tube in the form of pellets for interaction with the shock heated test gases.

2.3 Characterizations

Different experimental techniques were used to characterize the sample before and after exposure to shock heated test gases. Electronic structure of the ceramic was characterized by X-ray photoelectron spectroscopy (XPS) using Al Kα radiation (1486.6 eV) where C(1s) at 284.5 eV was taken as reference and the accuracy of the binding energy (BE) reported here was ±0.1 eV (MultiLab 2000, Thermo Fisher Scientific). X-ray diffraction (XRD) of the compound was recorded (Phillips X'Pert diffractometer) using Cu Kα radiation at scan rate of 0.25 (°)/min with 0.01° step size in the 2θ range between 20° and 80°. Fourier transform infrared (FTIR) spectra were recorded using FTIR spectrometer (Perkin Elmer, SPECTRUM-1000) in the 400–4000 cm^{-1} range by preparing KBr pellets. Scanning electron microscopy (SEM, Philips SIRION) and high resolution transmission electron microscopy (HRTEM, Technai T-20) operated at 200 kV were used to study the morphology and nano crystalline structure of CeO_2 before and after shock treatment.

3 Results and discussion

XPS spectra of Ce(3d) and N(1s) core levels of as-prepared and shock exposed CeO_2 are shown in Fig. 4. Ce($3d_{5/2}$) peak at 881.7 eV along with satellite peaks at 6.4 eV and 16 eV below the main peak is characteristic of Ce^{4+} in CeO_2 [23]. Characteristic satellite peak observed at 916.8 eV as shown in Fig. 4(i)(a) confirms that Ce is in 4+ state in this compound. After exposure to shock heated test gases like O_2 or N_2, BE of the main and satellite peaks of Ce(3d) remain the same as shown in Figs. 4(i)(b) and 4(i)(c) indicating that Ce is in 4+ state before and after exposure to shock heated gases. Thus, XPS results confirm no change in the electronic structure of CeO_2

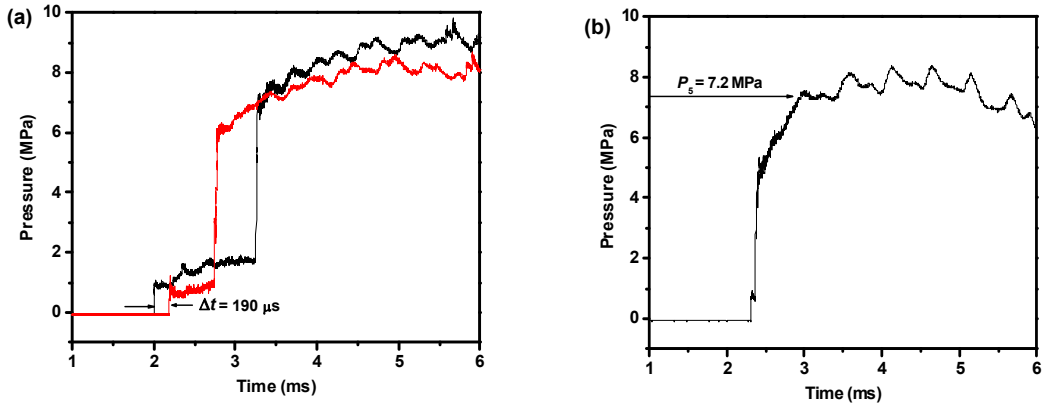

Fig. 3 Typical pressure signals acquired from pressure transducers: (a) time history data for the shock to travel 0.5 m distance; (b) reflected shock pressure (P_5) data.

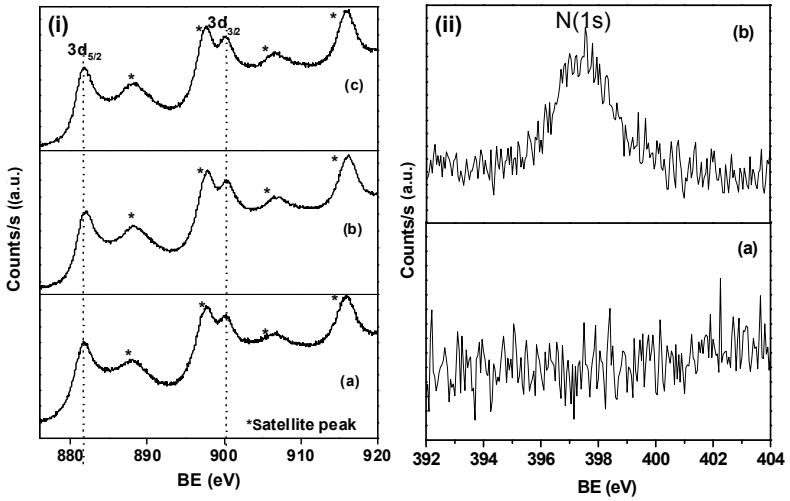

Fig. 4 (i) XPS spectra of Ce(3d): (a) as-prepared ceria ceramic, (b) after exposure to shock heated O_2 and (c) after exposure to shock heated N_2. (ii) XPS spectra of N(1s): (a) as-prepared sample and (b) after exposure to shock heated N_2.

in presence of shock heated O_2. Core level N(1s) spectra in CeO_2 before and after exposed to N_2 are shown in Fig. 4(ii). N(1s) peak is not observed in as-prepared CeO_2 sample as shown in Fig. 4(ii)(a). On the other hand, core level N(1s) peak at 397.5 eV after exposure to nitrogen is attributed to the formation of Ce–N bond due to the doping of nitrogen during shock treatment as shown in Fig. 4(ii)(b). XPS of N(1s) in nitrogen doped cerium in presence of NH_3 was reported in the literature [24]. The formation of $CeO_{2-x}N_x$ (nitrogen doped CeO_2) under strong shock compression is the signature of three-body non-catalytic surface reactions.

Powder XRD patterns of the nanoceramic CeO_2 before and after exposure to shock heated test gases are shown in Fig. 5. All the peaks are indexed into fluorite structure according to JCPDS No. 81-0792, and no impurity peak is detected in the XRD pattern of as-prepared CeO_2 given in Fig. 5(a). Thus, the compound explicitly crystallizes in fluorite structure (space group *Fm*3*m*, lattice parameter $a = 5.411$ Å). The diffraction lines are sharper and more intense in comparison with that of as-prepared ceramic due to melting and re-crystallization with increase in the size of crystallite. The characteristic diffraction lines are assigned with *hkl* values for CeO_2. XRD of CeO_2 ceramic remains cubic with increase in the intensity of diffraction lines after exposure to shock heated O_2 and N_2 as shown in Figs. 5(b) and 5(c). Also there is a clear shift of 0.3° towards the higher Bragg angle with the shock heated N_2 gas. With shock heated O_2 gas, the oxidation state of CeO_2 remains with Ce^{4+}, and Ce^{3+} can go to Ce^{4+} state. However there is no shift in the diffraction lines due to this process as shown in Fig. 5(b). During the interaction of CeO_2 with shock heated N_2, the oxide ion vacancies in the CeO_2 lattice due to Ce^{3+} ions are replaced by nitrogen atoms and form $CeO_{2-x}N_x$. Doping of nitrogen atoms to CeO_2 during shock compression reduces the lattice parameter by 0.033 Å with a clear shift of 0.3° towards higher angle in the diffraction lines as shown in Fig. 5(c). The study shows that there is no phase transformation of CeO_2 after subjecting CeO_2 to shock compression in presence of O_2 and N_2 gases.

FTIR spectra of as-prepared CeO_2 and the samples

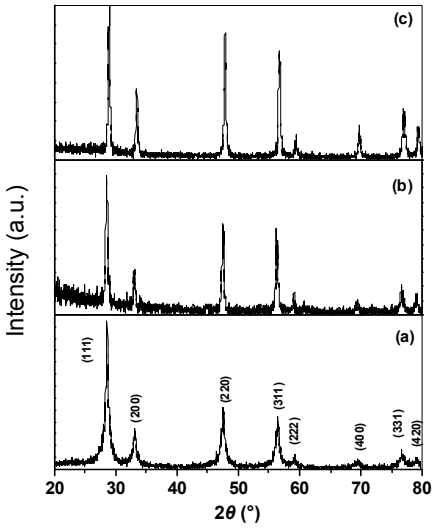

Fig. 5 XRD of CeO_2: (a) before exposure to shock, (b) after shock exposure to O_2 and (c) after shock exposure to N_2.

after shock exposure to O_2 and N_2 gases are shown in Figs. 6(a), 6(b) and 6(c), respectively. Small peaks at 2960 cm^{-1} and 2850 cm^{-1} are due to asymmetric stretching vibrations of $–CH_2$ bonds of glycine. The wide peak at 3000–3600 cm^{-1} range corresponds to –OH vibration band of H_2O present in the compound. The peaks around 3393 cm^{-1} and 1623 cm^{-1} are attributed to the O–H stretching and bending vibrations, respectively, and are in comparison with the literature [25,26]. There are shifts in O–H frequencies at 1623 cm^{-1} and 3393 cm^{-1} towards higher wavelength region after interaction with O_2. Peak around 3700 cm^{-1} as shown in Fig. 6(b) is due to bi- or tri-coordinated O–H species formed in presence of huge O_2 pressure during shock wave treatment [27]. The results demonstrate that as-prepared sample has absorbed H_2O molecules on the surface of CeO_2. The band at 1385 cm^{-1} is due to CO_2 present on the surface after exposure to shock heated O_2 gas. The absorption peaks of Ce–N and Ce–O bonding located at 900 cm^{-1} and 1150 cm^{-1} respectively indicate the presence of distinct nitrogen doped CeO_2 ($CeO_{2-x}N_x$) and CeO_2 phase as shown in Fig. 6(c). The main peak at 850–450 cm^{-1} is due to the presence of Ce–O bond.

SEM micrographs of ceramic CeO_2 samples before and after exposure to shock heated test gases are shown in Fig. 7 with 10000× magnification. Micrograph of CeO_2 before exposure to shock is shown in Fig. 7(a). When normal shock wave impinges on the sample for a short duration of 2–4 ms, the re-crystallization phenomenon spreads throughout the surface of the CeO_2 pellets. After exposure to shock heated O_2 and N_2 gases, the compound melts and the surface morphology of re-crystallized sample are shown in Figs. 7(b) and 7(c), respectively. During the exchange of lattice oxygen and formation of $CeO_{2-x}N_x$, pores and cracks of different sizes are developed on the surface of CeO_2 (Figs. 7(b) and 7(c)).

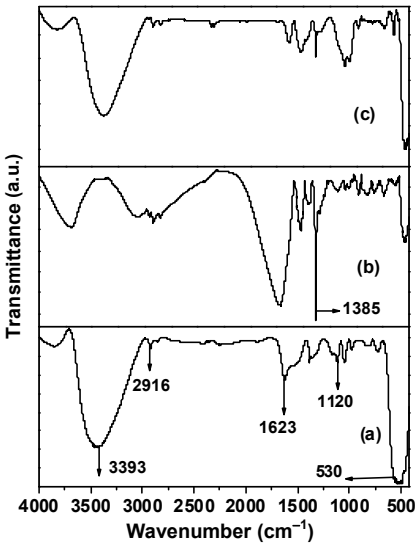

Fig. 6 FTIR spectra of CeO_2: (a) as-prepared sample, (b) after exposure to shock heated O_2 and (c) after exposure to shock heated N_2.

Bright field image, HRTEM image and electron diffraction pattern of as-prepared CeO_2 are shown in Fig. 8. Bright field image clearly shows that the sizes of ceramic crystallites are in the range of 10–15 nm as shown in Fig. 8(a). Ring type selected area electron diffraction pattern is indexed to fluorite structure which is shown in the inset of Fig. 8(a). Bright field image, HRTEM image and electron diffraction pattern of CeO_2 after exposure to shock heated O_2 gas are shown in Fig. 9. Crystallites are in the range of

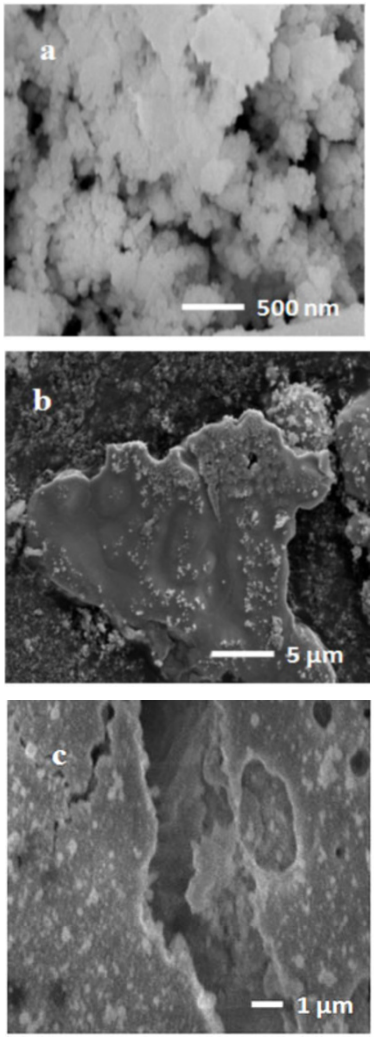

Fig. 7 SEM micrographs of CeO_2: (a) before shock, (b) after exposure to shock heated O_2 and (c) after exposure to shock heated N_2.

20–60 nm as evident from bright field image as shown in Fig. 9(a). This indicates that crystallite sizes are increased due to shock interaction. Electron diffraction pattern is indexed to fluorite structure and more intense bright spots are seen. Lattice fringe spacing of 3.11 Å is shown in Fig. 9(b), which corresponds to d_{111} plane of fluorite CeO_2 lattice (as shown in the inset of Fig. 9(a)). Bright field image, HRTEM image and electron diffraction pattern of CeO_2 after exposure to shock heated N_2 gas are shown in Fig. 10. Bright field image shows that crystallites are in the range of 20–80 nm, which indicates an increase in crystallite size. Electron diffraction shows clear rings with more intense bright spots, which are indexed to different crystal lattice. Lattice fringe spacing in HRTEM image is again 3.11 Å as shown in Fig. 10(b), which corresponds to d_{111} plane of fluorite CeO_2 lattice (as shown in the inset of Fig. 10(a)).

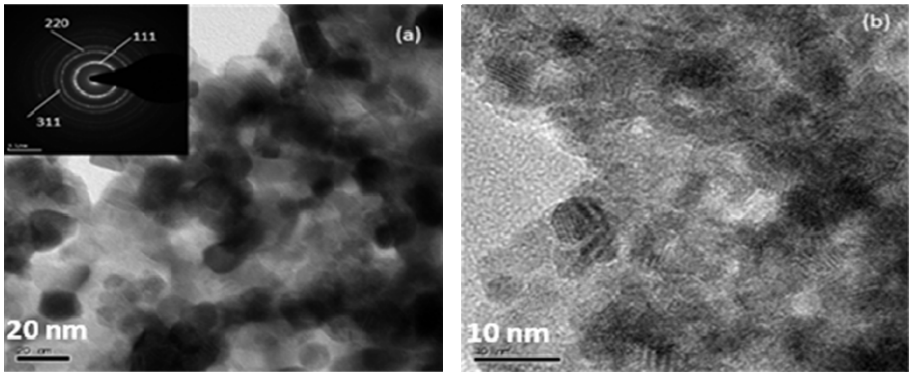

Fig. 8 As-prepared CeO_2 ceramic: (a) bright field image (inset: electron diffraction pattern) and (b) HRTEM image.

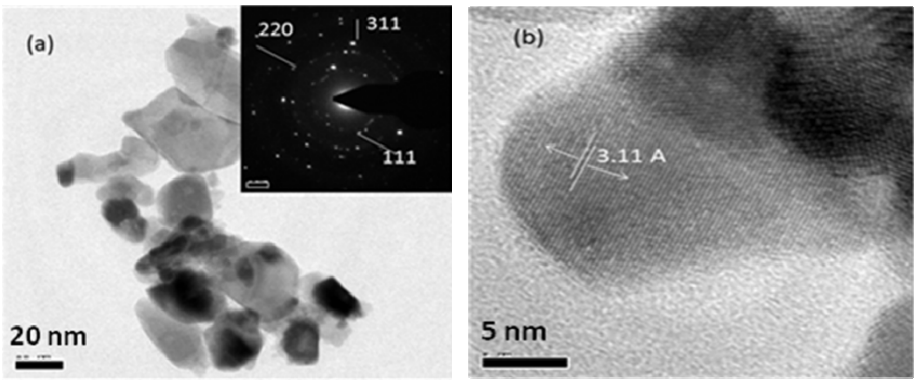

Fig. 9 CeO_2 sample after shock exposure to O_2: (a) bright field image (inset: electron diffraction pattern) and (b) HRTEM image.

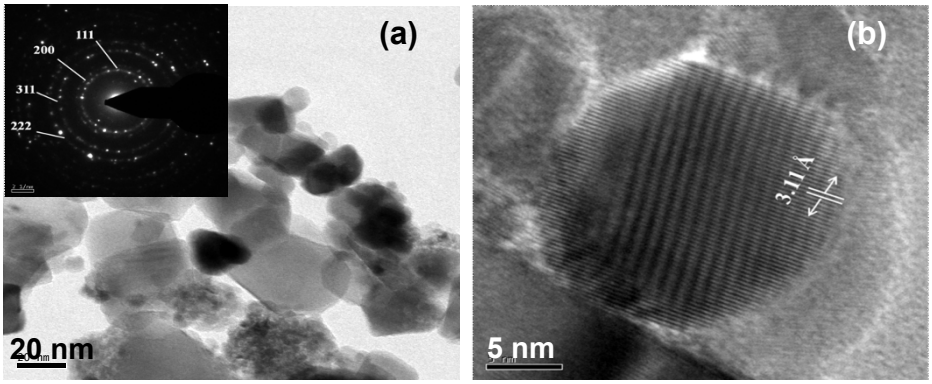

Fig. 10 CeO_2 sample after shock exposure to N_2: (a) bright field image (inset: electron diffraction pattern) and (b) HRTEM image.

CeO_2 undergoes three-body surface recombination reaction with non-dissociated and dissociated gas after shock treatment as follows.

(1) Reaction with non-dissociated and dissociated O_2 gas:

$$O_2 + M \rightarrow O_2 + M$$
$$O + O + M \rightarrow O_2 + M$$

In both the cases, the third body M (CeO_2) retains the same chemical composition and electronic structure. The crystal structure also remains as fluorite on shock loading. In practical applications, the extent of CeO_2 reduction occurring in the catalysis process is very small compared to complete reduction to Ce_2O_3 (or $CeO_{1.5}$). On shock heating $CeO_2 \rightarrow CeO_{2-\delta} + \delta/2O_2$ transformation takes place, where only partial oxygen vacancies are created by releasing lattice oxygen from CeO_2 by retaining its skeleton with fluorite structure.

(2) Reaction with non-dissociated and dissociated N_2 gas:

$$N_2 + M \rightarrow M_1$$
$$N + N + M \rightarrow M_1$$

In these cases, the third body M (CeO_2) will change to M_1 ($CeO_{2-x}N_x$) when oxygen vacancies are occupied by nitrogen atom. The chemical composition and electronic structure of new $CeO_{2-x}N_x$ were characterized by XRD, FTIR and XPS studies.

4 Conclusions

Shock-tube techniques are very useful to produce variable thermal shock for short duration at elevated pressure. Shock tubes are also used to study three-body catalytic and non-catalytic surface reactions with high enthalpy test gases. Three-body reactions were studied on ceramic CeO_2 sample with shock heated O_2 and N_2 test gases. The results obtained from different experimental techniques like XPS, XRD, FTIR, SEM and HRTEM show no change in the phase of CeO_2 before and after exposure to shock wave in the presence of O_2 gas. Further due to strong shock compression in the presence of N_2, the peak positions of diffraction lines are observed to be shifted equally towards the higher Bragg angle and XPS confirms that nitrogen is incorporated into the cubic fluorite structure. Nitrogen doped CeO_2 is also confirmed by FTIR studies through the characteristic Ce–N bond. SEM and HRTEM studies show increase in the crystallization of CeO_2 after shock treatment. The experimental results show the effect of strong shock heated gas interactions with CeO_2.

Acknowledgements

Financial supports for this study from the DST, DRDO and ISRO-IISc Space Technology Cell, Government of India, are gratefully acknowledged.

References

[1] Kim G. Ceria-promoted three-way catalysts for auto exhaust emission control. *Ind Eng Chem Prod Res Dev* 1982, **21**: 267–274.

[2] Bera P, Hegde MS. No reduction over noble metal ionic catalysts. *Catal Surv Asia* 2011, **15**: 181–199.

[3] Liao L, Mai HX, Yuan Q, *et al*. Single CeO_2 nanowire gas sensor supported with Pt nanocrystals: Gas sensitivity, surface bond states and chemical mechanism. *J Phys Chem C* 2008, **112**: 9061–9065.

[4] Pati RK, Lee IC, Chu D, *et al*. Nanosized ceria based water-gas shift (WGS) catalyst for fuel cell applications. *Prepr Pap-Am Chem Soc Div Fuel Chem* 2004, **49**: 953–954.

[5] Jain KK. Nanodiagnostics: Application of nanotechnology in molecular diagnostics. *Expert Rev Mol Diagn* 2003, **3**: 153–161.

[6] West JL, Halas NJ. Applications of nanotechnology to biotechnology: Commentary. *Curr Opin Biotech* 2000, **11**: 215–217.

[7] West JL, Halas NJ. Engineered nanomaterials for biophotonics applications: Improving sensing, imaging, and therapeutics. *Annu Rev Biomed Eng* 2003, **5**: 285–292.

[8] Yao HC, Yao YFY. Ceria in automotive exhaust catalysts: I. Oxygen storage. *J Catal* 1984, **86**: 254–265.

[9] Skorodumova NV, Simak SI, Lundqvist BI, *et al*. Quantum origin of the oxygen storage capability of ceria. *Phys Rev Lett* 2002, **89**: 166601.

[10] Skorodumova NV, Ahuja R, Simak SI, *et al*. Electronic, bonding, and optical properties of CeO_2 and Ce_2O_3 from first principles. *Phys Rev B* 2001, **64**: 115108.

[11] Gschneidner KA Jr, Eyring L. *Handbook on the Physics and Chemistry of Rare Earths*, *Volume 3*. Elsevier, 1979: 337.

[12] Xiao W, Tan D, Li Y, *et al*. The effects of high temperature on the high-pressure behavior of CeO_2.

J Phys: *Condens Matter* 2007, **19**: 425213.

[13] Jayaram V, Singh P, Reddy KPJ. Experimental investigation of nano ceramic material interaction with high enthalpy argon under shock dynamic loading. *Appl Mech Mater* 2011, **83**: 66–72.

[14] Jayaram V, Singh. P, Reddy KPJ. Study of anatase TiO_2 in the presence of N_2 under shock dynamic loading in a free piston driven shock tube. *Advances in Ceramic Science and Engineering* (*ACSE*) 2013, **2**: 40–46.

[15] Reddy NK, Jayaram V, Arunan E, *et al*. Investigations on high enthalpy shock wave exposed graphitic carbon nanoparticles. *Diam Relat Mater* 2013, **35**: 53–57.

[16] Vasu K, Matte HSSR, Shirodkar SN, *et al*. Effect of high-temperature shock-wave compression on few-layer MoS_2, WS_2 and $MoSe_2$. *Chem Phys Lett* 2013, **582**: 105–109.

[17] Patil KC, Hedge MS, Rattan T, *et al*. *Chemistry of Nanocrystalline Oxide Materials*: *Combustion Synthesis*, *Properties and Applications*. World Scientific, 2008: 119.

[18] Stalker RJ. A study of the free-piston shock tunnel. *AIAA J* 1967, **5**: 2160–2165.

[19] Kulkarni V, Hegde GM, Jagadeesh G, *et al*. Aerodynamic drag reduction by heat addition into the shock layer for a large angle blunt cone in hypersonic flow. *Phys Fluids* 2008, **20**: 081703.

[20] Jayaram V. Experimental investigations of surface interactions of shock heated gases on high temperature materials using high enthalpy shock tubes. Ph.D. Thesis. Indian Institute of Science, Bangalore, India, 2007.

[21] Reddy KPJ, Hedge MS, Jayaram V. Material processing and surface reaction studies in free piston driven shock tube. The 26th International Symposium on Shock Waves, Gottingen, Germany, 2007: 35–42.

[22] Gaydon AG, Hurle IR. *The Shock Tube in High Temperature Chemical Physics*. New York: The Reinhold Publishing Corporation, 1963: 23–28.

[23] Singh P, Hegde MS, Gopalakrishnan J. $Ce_{2/3}Cr_{1/3}O_{2+y}$: A new oxygen storage material based on the fluorite structure. *Chem Mater* 2008, **20**: 7268–7273.

[24] Jorge AB, Fraxedas J, Cantarero A, *et al*. Nitrogen doping of ceria. *Chem Mater* 2008, **20**: 1682–1684.

[25] Mokkelbost T, Kaus I, Grande T, *et al*. Combustion synthesis and characterization of nanocrystalline CeO_2-based powders. *Chem Mater* 2004, **16**: 5489–5494.

[26] Fu Y-P, Lin C-H, Hsu C-S. Preparation of ultrafine CeO_2 powders by microwave-induced combustion and precipitation. *J Alloys Compd* 2005, **391**: 110–114.

[27] Bera P, López-Cámara A, Hornés A, *et al*. Comparative *in situ* DRIFTS-MS study of ^{12}CO- and ^{13}CO-TPR on CuO/CeO_2 catalyst. *J Phys Chem C* 2009, **113**: 10689–10695.